

# Looking for a heavy wino LSP in collider and dark matter experiments

Utpal Chattopadhyay<sup>(a)</sup>, Debottam Das<sup>(a)</sup>, Partha Konar<sup>(b)</sup> and D.P.Roy<sup>(c,d)</sup>

<sup>(a)</sup>*Department of Theoretical Physics, Indian Association for the Cultivation of Science,  
Raja S.C. Mullick Road, Kolkata 700 032, India*

<sup>(b)</sup>*Institut für Theoretische Physik, Universität Karlsruhe, D-76128 Karlsruhe, Germany*  
<sup>(c)</sup><sup>1</sup>*Homi Bhabha Centre for Science Education, Tata Institute of Fundamental  
Research, Mumbai-400088, India*

<sup>(d)</sup>*Institute for Particle Physics Phenomenology, Ogden Centre for Fundamental Physics,  
Department of Physics, University of Durham, Durham DH1 3LE, United Kingdom*

## Abstract

We investigate the phenomenology of a wino LSP as obtained in AMSB and some string models. The WMAP constraint on the DM relic density implies a wino LSP mass of 2.0-2.3 TeV. We find a viable signature for such a heavy wino at CLIC, operating at its highest CM energy of 5 TeV. One also expects a viable monochromatic  $\gamma$ -ray signal from its pair-annihilation at the galactic centre at least for cuspy DM halo profiles.

## 1 Introduction

The minimal supersymmetric standard model (MSSM) is the most popular extension of the standard model (SM) on account of four attractive features [1]. It provides (1) a natural solution to the hierarchy problem of the SM, (2) a natural (radiative) mechanism for the electroweak symmetry breaking (EWSB) , (3) a natural candidate for the cold dark matter (DM) of the universe in the form of the lightest superparticle (LSP), a prediction that has gained in importance in view of recent observations [2], and (4) unification of the SM gauge couplings at the GUT scale. However it also suffers from two problems:

(i) Little Hierarchy Problem: The LEP limit on the mass of an SM-like Higgs boson [3],

$$m_h > 114 \text{ GeV}, \quad (1)$$

---

<sup>1</sup>Permanent Address

requires the average top squark mass to be typically an order magnitude higher than  $M_Z$  [4]. This implies some fine-tuning of SUSY parameters to obtain the correct value of  $M_Z$ .

(ii) Flavour and CP Violation Problem: The general MSSM makes fairly large 1-loop contributions to flavour changing neutral current (FCNC) processes, like  $\mu \rightarrow e\gamma$  decay, as well as to CP violating processes like fermion electric dipole moments (EDM). The experimental limits on these FCNC decays require either large scalar masses,

$$m_\phi \gtrsim 10 \text{ TeV} \quad (2)$$

or a near degeneracy among the sfermion masses of different generations. Similarly, the experimental limits on the electron and neutron EDM require either large scalar masses (as in Eq.2) or unnaturally small CP violating phases. It may be added here that while the degeneracy of sfermion masses can be realised in simple models like minimal supergravity (mSUGRA) or anomaly mediated SUSY breaking (mAMSB), there is no simple model ensuring small SUSY phases.

The split SUSY model [5] tries to solve the second problem at the cost of aggravating the first by pushing up the scalar superparticle masses. In fact the cost is much more, since this model assumes the scalar masses to be many orders of magnitude larger than the TeV scale. This means that one has to give up (1) the supersymmetric solution to the hierarchy problem of the SM along with (2) the radiative EWSB mechanism. One only retains the LSP dark matter and the unification of gauge couplings, since the chargino and the neutralino masses are assumed to remain within a few TeV. We find the cost much too high since the first two features were the original motivations for weak scale supersymmetry.

We shall consider instead a more conservative model where the scalar superparticle masses are assumed to lie in the range

$$m_\phi = 10 - 100 \text{ TeV}. \quad (3)$$

Thus, it solves the second problem at the cost of aggravating the first; but without abandoning the supersymmetric solution to the hierarchy problem or the radiative EWSB mechanism. Moreover, we retain the LSP dark matter as well as gauge coupling unification by assuming the chargino and neutralino masses to remain within a few TeV.

We shall be primarily interested in the electroweak chargino-neutralino sector and in particular the lightest neutralino, which we assume to be the LSP. The diagonal elements of the  $4 \times 4$  neutralino mass matrix are  $M_1$ ,  $M_2$ , and  $\pm\mu$ , corresponding to the bino  $\tilde{B}$ , the wino

$\tilde{W}$ , and the higgsinos  $\tilde{H}_{1,2} = \tilde{H}_u \pm \tilde{H}_d$ , respectively, while the non-diagonal elements are all  $\leq M_Z$ . Now, there are experimental indications from the Higgs mass limit (Eq. 1) and the  $b \rightarrow s\gamma$  decay width that the SUSY masses representing the above diagonal elements are typically larger than  $M_Z$ , at least in a universal MSSM like the mSUGRA model [6]. We shall assume this mass inequality to hold in a more general MSSM. Then it implies that the neutralino mass eigenstates correspond approximately to the above interaction eigenstates  $\tilde{B}$ ,  $\tilde{W}$  and  $\tilde{H}_{1,2}$  and the LSP constitutes of one of these states. An interesting exception to this rule is provided by the case of a near degeneracy between two diagonal elements, which results in a large mixing between the corresponding interaction eigenstates, as the mixing angle is given by  $\tan 2\theta = 2 M_{ij} / |M_{ii} - M_{jj}|$ . In particular the LSP can be a mixed bino-higgsino, bino-wino or wino-higgsino state. Such mixed LSP cases have been investigated in Ref. [7, 8], and named “well-tempered” neutralino in Ref. [8].

Leaving aside such an accidental degeneracy between the two lightest mass eigenvalues, one expects the LSP to be approximated by one of the interaction states - bino, wino or higgsino. The bino carries no gauge charge and hence does not couple to gauge bosons. Thus it can only pair-annihilate via sfermion exchange. But the current experimental lower limits on the sfermion masses [3] imply a low annihilation rate, resulting in an overabundance of dark matter over most of the MSSM parameter space. Only in special regions like stau co-annihilation ( $M_1 \simeq m_{\tilde{\tau}_1}$ ) or resonant pair annihilation ( $2M_1 \simeq m_A$ ) can one get a cosmologically acceptable DM relic density. But neither of these regions extend to the scalar mass range of Eq.(3). Even the so called focus point region, which corresponds to a “well-tempered” bino-higgsino LSP, does not reach the scalar mass range of Eq.3 in the universal MSSM [9, 10], although, in a generic and unconstrained MSSM, it can obtain the correct DM relic density for very large scalar masses [8]. In contrast, the higgsino and wino carry isospins 1/2 and 1 respectively. Hence they can pair annihilate to

$$\tilde{H}\tilde{H} \rightarrow WW(\bar{f}f), \quad \tilde{W}\tilde{W} \rightarrow WW(\bar{f}f), \quad (4)$$

by their gauge couplings to W boson. Consequently, the annihilation rate and the resulting DM relic density is controlled mainly by the higgsino (wino) LSP mass. It has only a marginal dependence on the sfermion mass [8] and it is practically independent of the other SUSY parameters. The current WMAP result on the DM relic density alongwith the  $2\sigma$  error bar [11] is

$$\Omega_{\tilde{\chi}} h^2 = 0.104^{+0.015}_{-0.019} \quad (5)$$

where  $h = 0.73 \pm 0.03$  is the Hubble constant in units of  $100 \text{ Km s}^{-1} \text{ Mpc}^{-1}$  [11] and  $\Omega_{\tilde{\chi}}$  is the DM relic density in units of the critical density. This corresponds to a higgsino (wino) LSP mass of about 1 (2) TeV, where the larger wino mass is due to its larger gauge coupling. In ref. [10] we investigated the phenomenology of higgsino LSP in collider and dark matter experiments. The present work is devoted to a similar investigation for the wino LSP.

In the next section, we discuss the wino LSP models and estimate the wino mass band compatible with the WMAP relic density range of Eq.5 . In the two following sections we investigate the prospects of detecting such a heavy wino LSP in future collider and DM search experiments respectively. Finally we shall conclude with a summary of our results.

## 2 Wino LSP in AMSB and string models:

A universal gaugino mass at the GUT scale leads to the weak scale wino being always heavier than the bino, since the gaugino masses evolve like the corresponding gauge couplings. Hence, the wino LSP scenario can not be realised in the universal MSSM. The most popular SUSY model for a wino LSP is the anomaly mediated supersymmetry breaking (AMSB) model [12,13] wherein the gaugino and scalar masses arise from supergravity breaking in the hidden sector via super-Weyl anomaly contributions [14], namely,

$$M_\lambda = \frac{\beta_g}{g} m_{3/2} \quad (6)$$

$$m_\phi^2 = -\frac{1}{4} \left( \frac{\partial \gamma}{\partial g} \beta_g + \frac{\partial \gamma}{\partial y} \beta_y \right) m_{3/2}^2 \quad (7)$$

$$A_y = -\frac{\beta_y}{y} m_{3/2}. \quad (8)$$

Here  $m_{3/2}$  is the gravitino mass,  $\beta_g$  and  $\beta_y$  are the  $\beta$  functions for gauge and Yukawa couplings, and  $\gamma = \partial \ln Z / \partial \ln \mu$ , where  $Z$  is the wave function renormalization constant. The GUT scale gaugino masses (6) are thus non-universal, with

$$M_1 = \frac{33}{5} \frac{g_1^2}{16\pi^2} m_{3/2}, \quad M_2 = \frac{g_2^2}{16\pi^2} m_{3/2}, \quad M_3 = -3 \frac{g_3^2}{16\pi^2} m_{3/2} \quad (9)$$

at the one loop level. Evolving down to the weak scale gives

$$M_1 : M_2 : |M_3| \simeq 2.8 : 1 : 7.1 \quad (10)$$

including the two loop corrections. Unfortunately, evolving the scalar masses of Eq.(7) down to the weak scale gives negative mass-square values for sleptons. In the minimal version of the model (mAMSB) this is remedied by adding a common parameter  $m_0^2$  to the right hand side of Eq.(7) for all the scalars in the theory. This model has been widely studied because of its economy of parameters, *i.e.*,

$$m_{3/2}, m_0, \tan \beta, \text{sgn}(\mu) \quad (11)$$

$\mu^2$  being fixed by the radiative EWSB condition. We shall come back to this model below.

It should be noted here that the anomaly mediated contributions of Eqs.(6,7,8) are present in all supergravity models. But, in general, one can also have tree level SUSY breaking contributions to the gaugino and scalar masses arising from possible dimension five and six terms in the effective Lagrangian, namely

$$m_\lambda \in \frac{F_S}{M_{pl}} \lambda \lambda \quad (12)$$

and

$$m_\phi^2 \in \frac{F_S^\dagger F_S}{M_{pl}^2} \phi^* \phi \quad (13)$$

where  $F_S$  is the vev of the  $F$  component of a chiral superfield  $S$  responsible for SUSY breaking. If present, these tree level contributions are expected to overwhelm the anomaly mediated contributions of Eqs.(6& 7). The AMSB scenario assumes the SUSY breaking superfield to be carrying a non-zero gauge charge, so that the gaugino mass term (Eq.12) is eliminated by gauge symmetry. However, such symmetry considerations can not eliminate the tree level scalar mass term (Eq.13). So in this case the scalar mass is expected to be typically larger than the gaugino mass by a loop factor, namely

$$m_\phi \sim 100 M_\lambda . \quad (14)$$

This was the case in the AMSB model of Ref. [13] which has been revived in Ref. [15]. On the other hand, the mAMSB model [12, 14] assumes the SUSY-breaking hidden sector and the visible sector to reside on two different branes, separated by a large distance in a higher dimensional space, so that the tree level scalar mass term (Eq.13) is suppressed by geometric considerations. We shall consider both the possibilities here.

Note also that one can get a AMSB like scenario in the string theory, where the tree-level SUSY breaking masses can only come from the dilaton field, while they receive only loop

contributions from moduli fields. In fact, such a scenario was already suggested in Ref. [16] before the AMSB model by assuming that SUSY breaking is dominated by a modulus field. It contributes to the gaugino mass  $M_\lambda$  as well as the squared scalar mass  $m_\phi^2$  at the 1-loop level. The resulting hierarchy of gaugino masses is very similar to that of the AMSB (9). On the other hand, the scalar mass here is expected to be typically larger than the gaugino mass by the square root of the loop factor, *i.e.*

$$m_\phi \sim 10M_\lambda. \quad (15)$$

Note that the range (3) is roughly compatible with both Eqs.(14 & 15).

As mentioned earlier, we expect the DM relic density to be determined by the wino mass  $M_2$ , practically independent of the other model parameters. To check this, we have computed the DM relic density, using the *Micromegas* code [17], as a function of  $M_2$  with the corresponding  $M_1$  and  $M_3$  determined from the AMSB relation (Eq.10). With the above gaugino mass relation, the wino mass values for the three values (lower, central and upper) of the WMAP relic density of Eq.(5) corresponding to a common sfermion mass of 10 TeV are

$$(M_2, \Omega_{\tilde{\chi}} h^2) : \quad (1.91 \text{ TeV}, 0.084), (2.10 \text{ TeV}, 0.104), (2.23 \text{ TeV}, 0.119). \quad (16)$$

The other chosen SUSY parameters were  $\mu = 9$  TeV and  $\tan \beta = 10$ . In other words, the wino mass range corresponding to the  $\pm 2\sigma$  range of the WMAP relic density is

$$M_2 \simeq 1.9 - 2.2 \text{ TeV}. \quad (17)$$

We have confirmed these results using the DARKSUSY code [18] and cross checked them with the results obtained by Profumo [19]. We have also checked that changing the sfermion mass from 10 to 100 TeV changes the wino mass upper limit of (16) from 2.23 to 2.37 TeV, due to the vanishing of the small but negatively interfering sfermion contribution, while it has practically no dependence on  $\mu$  and  $\tan \beta$ .

We have also done a more detailed analysis using the mAMSB model. We have estimated the weak scale superparticle masses from the GUT scale input parameters (11) via two loop RGE using the SUSPECT code [20]. The superparticle masses were then used in the *Micromegas* to compute the DM relic density.

Fig. 1 shows the allowed parameter space in the  $m_{3/2} - m_0$  plane for  $\tan \beta = 10$  and positive  $\mu$ . The upper disallowed region corresponds to  $\mu^2 < 0$ , *i.e.* no radiative EWSB,

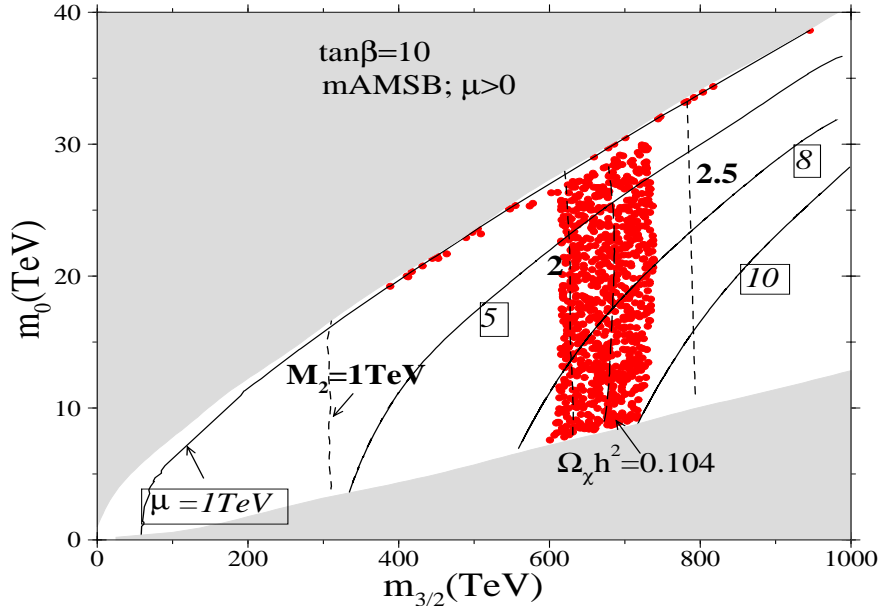


Figure 1: Allowed and disallowed regions of the mAMSB parameter space with contours shown for  $\mu$  (solid lines) and  $M_2$  (dashed lines). The WMAP satisfied neutralino relic density zone is shown by red/dark dots which is concentrated in the region of  $M_2 = 2.0 - 2.3$  TeV. A contour for  $\Omega_{\tilde{\chi}} h^2 = 0.104$  (central value) is also shown. Isolated dots near the REWSB boundary correspond to Higgsino dominated LSP regions. The upper shaded (gray) region is disallowed via  $\mu^2 < 0$ , *i.e.* the first REWSB constraint. The lower shaded (gray) region is disallowed as it contains a tachyonic slepton zone (for smaller  $m_{3/2}$ ) and a tachyonic pseudoscalar Higgs zone (for larger  $m_{3/2}$ ), *i.e.* from the second REWSB constraint.

while the lower disallowed region corresponds to either a tachyonic slepton (for small  $m_{3/2}$ ) or a tachyonic pseudoscalar Higgs (larger  $m_{3/2}$ ). It also shows contours of fixed  $\mu$  and fixed  $M_2$  in the allowed region of parameter space. The dotted band shows the part compatible with the WMAP relic density range of eq.(5), that is the wino mass band

$$M_2 = 1.9 - 2.3 \text{ TeV.} \quad (18)$$

Note also a thin dotted band around the  $\mu = 1$  contour, representing a higgsino LSP. Thus, a WMAP satisfying higgsino LSP of mass of  $\sim 1$  TeV is realised in mAMSB as well as in the mSUGRA model [10]. The lower end of wino mass corresponds to slepton and squark masses in the range of  $9 - 14$  TeV, while the upper end corresponds to these masses in

the range of  $28 - 30$  TeV. All these results are very insensitive to changes in  $\tan\beta$  and  $\text{sign}(\mu)$ . It should be noted here that the region below the WMAP compatible wino mass band of Eq.18 corresponds to an under-abundance of the DM relic density in the standard cosmological model. This region may be allowed if there are alternative DM candidates, or, more interestingly, if there are non-standard cosmological mechanisms for enhancing the relic density of the wino DM. In fact, both thermal and non-thermal mechanisms for enhancing the wino relic density have been suggested in the literature [21, 22]. In the first case, the presence of a quintessence field leads to faster Hubble expansion and hence an earlier freeze-out, resulting in a higher thermal relic density [21]. In the second case, late decay of the gravitino enhances the wino relic density in the AMSB model [14, 22]. Therefore, while investigating the wino LSP signal in collider and dark matter search experiments in the next two sections we shall cover wino masses below the band of Eq.18 as well.

### 3 Wino LSP search in collider experiments

Evidently, the wino mass band of Fig. 1 is way above the discovery reach of LHC in the AMSB model [23]. In fact, the total wino pair production cross-section at LHC ( $\tilde{W}^\pm\tilde{W}^0 + \tilde{W}^+\tilde{W}^-$ ) is only  $\sim 10^{-2}$  fb [7], corresponding to 1 event per year even at the high luminosity run of LHC. Moreover, the mass degeneracy of  $\tilde{W}^\pm$  and  $\tilde{W}$  implies that the only visible objects in the final state will be 1 or 2 soft pions from the

$$\tilde{W}^\pm \rightarrow \pi^\pm \tilde{W}^0 \quad (19)$$

decay. It will be impossible to identify such events without an effective tag at the LHC.

The most promising machine for detecting a wino LSP of mass up to the 2 TeV range is the proposed  $e^+e^-$  linear collider CLIC, operating at its highest energy of 5 TeV [24]. We shall follow the strategy of Ref. [25] in estimating the signal and the background. The same strategy has been followed by the LEP experiments in setting mass limits on a wino LSP [3]; in particular, the OPAL experiment has used it to set a mass limit of 90 GeV [26]. The pair production of charged wino is tagged by a hard photon from initial state radiation (ISR), *i.e.*

$$e^+e^- \rightarrow \gamma\tilde{W}^+\tilde{W}^-. \quad (20)$$

The photon is required to have an angle

$$170^\circ > \theta_\gamma > 10^\circ \quad (21)$$

relative to the beam axis. Moreover, it is required to satisfy

$$E_T^\gamma > E_T^{\gamma_{min}} = \sqrt{s} \frac{\sin \theta_{min}}{1 + \sin \theta_{min}} = 100 \text{ GeV}, \quad (22)$$

which vetoes the radiative Bhaba background  $e^+e^- \rightarrow \gamma e^+e^-$ , by kinematically forcing one of the energetic  $e^\pm$  to emerge at an angle  $> \theta_{min}$ . At the maximum CLIC energy of  $\sqrt{s} = 5$  TeV, the above  $E_T^{\gamma_{min}}$  of 100 GeV implies  $\theta_{min} \simeq 1.2^\circ$ . The OPAL detector has instrumentation down to  $\theta_{min} = 2^\circ$ , while it seems feasible to extend it down to  $1^\circ$  at future linear colliders [25]. We shall also impose the recoil mass cut

$$M_{rec} = \sqrt{s} \left( 1 - \frac{2E_T^\gamma}{\sqrt{s}} \right)^{\frac{1}{2}} > 2m_{\tilde{\chi}}, \quad (23)$$

where  $m_{\tilde{\chi}}$  represents the LSP mass ( $= M_2$  for wino). This is automatically satisfied by the signal (Eq.20).

In calculating the cross-section of Eq.20 we have included ISR effects by convoluting the hard  $2 \rightarrow 3$  cross-section with the electron distribution function as described in Ref. [27]. Although a negatively interfering  $t$ -channel  $\tilde{\nu}_e$  exchange contribution reduces the above cross-section for smaller sneutrino masses, the decrease is  $\lesssim 15\%$  for our region of interest (Eq.3) where sfermion mass is higher than 10 TeV. Hence, we have neglected the sneutrino exchange contribution.

If we can not identify the  $\tilde{W}^\pm \rightarrow \tilde{W}^0$  decay products then the main background is

$$e^+e^- \rightarrow \gamma \nu \bar{\nu}. \quad (24)$$

Fig.2 shows the signal and background cross-sections as function of the LSP mass. The latter is seen to be larger by a factor of  $\sim 1000$  owing to the large contribution from the  $t$ -channel  $W$ -exchange contribution to  $\gamma \nu_e \bar{\nu}_e$  production. In the case of higgsino LSP signal, this background could be suppressed by using right (left) polarised  $e^-$  ( $e^+$ ) beam [10]. Unfortunately, this does not help here since the wino pair production signal (20) can arise only from the left (right) polarised  $e^-$  ( $e^+$ ) collision. On the other hand, one can enhance the signal cross-section along with the background by using left (right) polarised  $e^-$  ( $e^+$ )

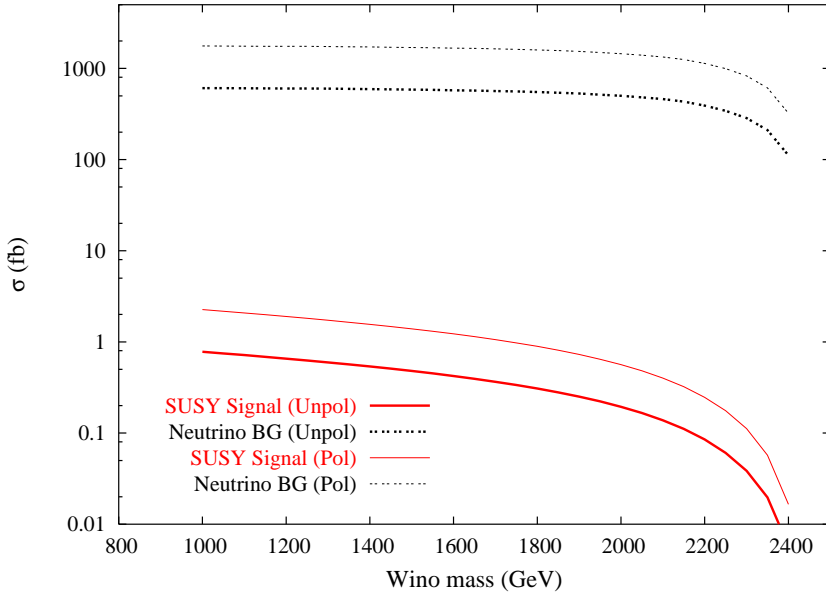


Figure 2: Cross-sections for the wino signal (solid) and the neutrino background (dashed) at CLIC ( $\sqrt{s} = 5$  TeV) with both unpolarised (thick lines) and polarised (thin lines)  $e^-$  and  $e^+$  beams. Initial state radiation is included.

beam. We have estimated the signal and background cross-sections for beam polarisations similar to that envisaged for ILC [28], *i.e.*

$$P_{e^-} = -0.8 \text{ (mostly left handed)}, P_{e^+} = 0.6 \text{ (mostly right handed)}. \quad (25)$$

It is easy to check that it corresponds to the following fractional luminosities,

$$e_L^- e_R^+ : e_R^- e_L^+ : e_R^- e_R^+ : e_L^- e_L^+ = 0.72 : 0.02 : 0.08 : 0.18 \quad (26)$$

while each was 0.25 in the unpolarised case. It results in increase of both the signal and the background cross-sections by a factor of  $0.72/0.25 \simeq 3$ , as shown in Fig. 2.

Evidently, it is essential to identify the  $\tilde{W}^\pm \rightarrow \tilde{W}^0$  decay products for extracting the signal (Eq.20) from the much larger background (Eq.24). Indeed it is possible to identify these decay products unambiguously unlike those for the higgsino case [10], thanks to a robust prediction for the  $\tilde{W}^\pm$  and  $\tilde{W}^0$  mass difference  $\delta m$  [14, 29], which largely arises from radiative corrections. The gauge boson loops give [30]

$$\delta m = \frac{\alpha M_W}{2(1 + \cos \theta_W)} \left[ 1 - \frac{3}{8 \cos \theta_W} \frac{M_W^2}{M_2^2} \right] \simeq 165 \text{ MeV} \quad (27)$$

with the approximate equality holding only for  $\mu \gg M_2 \gg M_W$ . For  $M_2 \sim 2$  TeV and  $\mu > M_2$ , the region of our interest, it gives

$$\delta m = 165 - 190 \text{ MeV}. \quad (28)$$

The tree-level contribution to  $\delta m$  is  $\simeq \tan^2 \theta_W \sin^2 2\beta M_W^4 / (M_1 \mu^2) < 1$  MeV. Similarly, the sfermion exchange loop contribution to  $\delta m$  is  $\mathcal{O}(M_W^4/m_\phi^3) < 1$  MeV.

The mass difference of Eq.(28) implies  $\tilde{W}^\pm \rightarrow \pi^\pm \tilde{W}^0$  to be the dominant decay mode with a range  $c\tau = 3 - 7$  cm, nearly independent of the wino mass [25]. Moreover, as was pointed out in [25], the SLD vertex detector has its innermost layer at 2.5 cm from the beam and this gap is proposed to be reduced to 2 cm or even less at the future linear colliders. Thus, it should be possible to observe the tracks of  $W^\pm$  as two heavily ionising particles along with their decay  $\pi^\pm$  tracks in vertex detector. Moreover for the momentum of the decay pion,  $p_\pi \sim \sqrt{\delta m^2 - m_\pi^2} \sim 87 - 128$  MeV, one expects the impact parameter resolution to be better than 0.3 mm. Thus both the decay pions have impact parameters of  $\gtrsim 100\sigma$ , which should be easily measurable. These should enable us to distinguish the signal (Eq.20) unambiguously from the background (Eq.24) even in the presence of the beamstrahlung pions [31]. Therefore we expect the viability of the signal to be determined primarily by the number of signal events.

We see from Fig. 2 that, with the proposed luminosity of  $1000 fb^{-1}$  at CLIC [24], one expects 600 (200) to 120 (40) events with polarised (unpolarised) beams for the WMAP satisfying wino mass range of 2.0 to 2.3 TeV (18). It should be noted here that the search can be extended to wino mass of 2.4 (2.5) TeV with a proportionate increase of the beam energy by 5 (10)%.

Fig. 3 shows the recoil mass distribution of a 2 TeV wino LSP signal along with the background events. While the recoil mass distribution of the background (24) stretches all the way from  $M_Z$  up to the kinematic limit, the signal shows a characteristic threshold at  $2m_{\tilde{\chi}}$ . This will help confirm the signal as well as to measure the LSP mass  $m_{\tilde{\chi}}$ .

## 4 Wino LSP search in DM experiments

The wino LSP signal is too small to be observed in direct dark matter search experiments. The reason is that this signal comes from spin-independent  $\tilde{\chi}p$  scattering, which is dominated

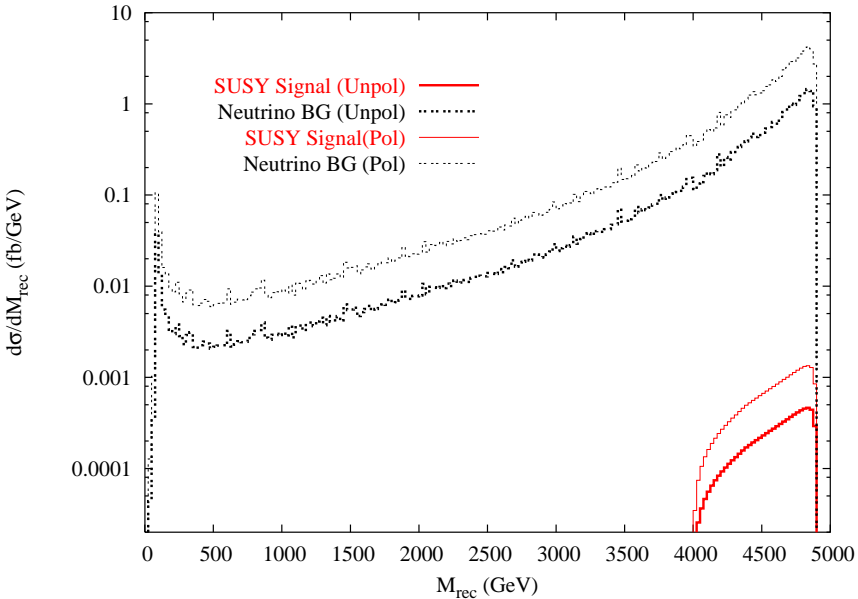


Figure 3: Recoil mass distributions of a 2 TeV wino signal and the neutrino background at CLIC ( $\sqrt{s} = 5$  TeV) with both unpolarised (thick lines) and polarised (thin lines)  $e^-$  and  $e^+$  beams. Initial state radiation is included.

by Higgs boson( $h, H$ ) exchange. Since the Higgs coupling to the LSP pair is proportional to the product of their higgsino and gaugino components, it is vanishingly small for the wino LSP. The signal is further suppressed by the large LSP mass. Likewise, the neutrino signal coming from the pair annihilation of wino LSP in the solar core is vanishingly small. This is because the solar capture rate of the LSP is controlled by the spin-dependent  $\tilde{\chi}p$  scattering cross-sections via  $Z$  boson; and the  $Z$  coupling to  $\tilde{\chi}$  pair is proportional to the square of its higgsino component.

The most promising wino DM signal is expected to come from  $\gamma$ -rays produced by its pair annihilation at the galactic centre. The largest signal comes from the tree-level annihilation process (4) into  $WW$ , followed by the decay of the  $W$  into  $\gamma$ -rays via neutral pions [7]. Unfortunately, the continuous energy spectrum of the resulting  $\gamma$ -rays suffers from a large background from the cosmic-ray pions. We consider instead the monochromatic  $\gamma$ -ray signal coming from the annihilation process

$$\tilde{W}\tilde{W} \rightarrow \gamma\gamma, \gamma Z \quad (29)$$

via  $\tilde{W}^\pm W^\mp$  loops [32]. For the resulting cross-sections,

$$v\sigma_{\gamma\gamma} \sim v\sigma_{\gamma Z} \sim 10^{-27} \text{ cm}^3 \text{ s}^{-1}, \quad (30)$$

where  $v$  is the velocity of the DM particles in their cms frame. The resulting  $\gamma$ -ray flux coming from an angle  $\psi$  relative to the galactic centre can be written as [32]

$$\Phi_\gamma(\psi) = 1.87 \times 10^{-13} \frac{N_\gamma v \sigma}{10^{-27} \text{ cm}^3 \text{ s}^{-1}} \left( \frac{1 \text{ TeV}}{m_{\tilde{\chi}}} \right)^2 J(\psi) \text{ cm}^{-2} \text{ s}^{-1} \text{ sr}^{-1} \quad (31)$$

where  $N_\gamma = 2$  (1) for the  $\gamma\gamma$  ( $\gamma Z$ ) production; and

$$J(\psi) = \frac{\int_{line \ of \ sight} \rho^2(\ell) d\ell(\psi)}{[(0.3 \text{ GeV/cm}^3)^2 \cdot 8.5 \text{ kpc}]} \quad (32)$$

is the line integral of the squared DM energy density scaled by its local value in our neighbourhood and our distance from the galactic centre.

Several Atmospheric Cerenkov Telescopes (ACT) have started recording TeV scale  $\gamma$ -rays from the galactic center e.g. HESS and CANGAROO in the southern hemisphere and MAGIC and WHIPPLE in the north. One generally expects concentration of DM in the galactic centre; but its magnitude has a large uncertainty depending on the assumed profile of DM halo density distribution [33–35]. The cuspy NFW profile [33] corresponds to

$$\langle J(0) \rangle_{\Delta\Omega=10^{-3}} \simeq 1000, \quad (33)$$

which represents the DM flux in the direction of the galactic centre averaged over the typical ACT aperture of  $\Omega = 10^{-3}$  sr. Extreme distributions, like the spiked profile [34] and core profile [35], correspond respectively to increase and decrease of this flux by a factor of  $10^3$ . We have computed the  $\gamma$ -ray line signal (31) in the mAMSB model for the NFW profile and an aperture  $\Delta\Omega = 10^{-3}$  sr using the DARKSUSY code [18]. Fig. 4 shows the resulting signal against the LSP mass, where we have added the  $\gamma\gamma$  and  $\gamma Z$  contributions, since they give identical photon energy ( $= m_{\tilde{\chi}}$ ) within the experimental resolution. The points satisfying WMAP relic density are shown as bold dots. One clearly sees a wino LSP of 2-2.3 TeV mass predicting a line  $\gamma$ -ray flux of  $\sim 10^{-13} \text{ cm}^{-2} \text{ s}^{-1}$  along with a higgsino LSP of 1 TeV mass predicting a flux of  $\sim 10^{-14} \text{ cm}^{-2} \text{ s}^{-1}$ . Both these are in agreements with the results of reference [29] and [36]. They are within the detection range of the above-mentioned ACT experiments. In particular, the wino signal has the advantage of an order of magnitude

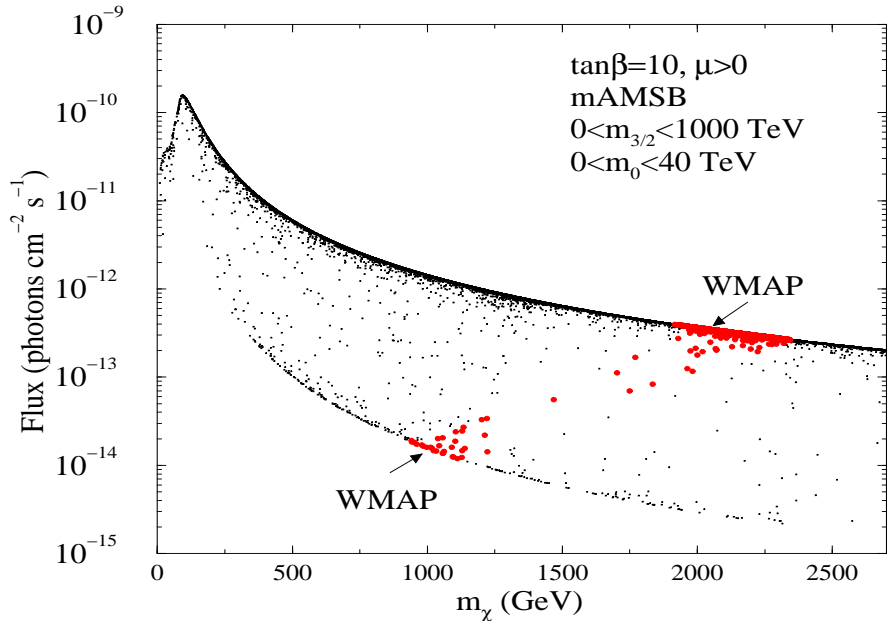


Figure 4: Monochromatic  $\gamma$ -ray flux from LSP pair annihilation at the galactic center for the NFW profile of DM halo distribution with an aperture of  $\Delta\Omega = 10^{-3}$  sr for mAMSB model for varying LSP mass. The red (darker) points correspond to the WMAP relic density satisfied values of eq.5

higher flux compared to the higgsino LSP. Furthermore, its higher mass implies an order of magnitude lower background from cosmic-ray proton and electron showers, as shown in Ref. [36]. It is further shown in [36] that one expects to see a  $5\sigma$  wino signal over this background at these ACT experiments for a NFW (or cuspier) profile.

However, it should be noted here that the HESS experiment has reported TeV photons coming from the direction of the galactic centre with an energy spectrum, which is unlike that expected from a TeV scale  $\gamma$ -ray line [37]. Instead, it shows a power law decrease with energy, which is similar to that of other "cosmic accelerators", notably the supernova remnants (SNR). Besides this, it is not clear whether this signal is coming right from our galactic centre (defined as the location of the super-massive black hole Sagittarius  $A^*$ ), or from a nearby SNR lying within the angular resolution of HESS. In particular, the SNR Sagittarius  $A$  east, lying a few parsecs away from Sagittarius  $A^*$  has been suggested to be the culprit [38]. Given the modest energy resolution of the present ACT experiments ( $\sim 15\%$ ), it may be more difficult to extract a line  $\gamma$  ray signal at the  $5\sigma$  level in the presence of this

$\gamma$  ray background. Therefore it is imperative to improve the energy and angular resolution of these experiments to suppress this background; and also to look for other possible clumps of DM in galactic halo [39].

## 5 Summary

- 1) We study the phenomenology of a wino LSP obtaining in the AMSB and some string models.
- 2) The WMAP constraint on the DM relic density implies a heavy wino LSP mass of  $2.0 - 2.3$  TeV in the standard cosmology. But one can also have wino LSP mass  $< 2$  TeV assuming nonstandard cosmological mechanisms for enhancing the DM relic density.
- 3) We find a viable wino LSP signal all the way upto 2.3 TeV at the proposed  $e^+e^-$  linear collider (CLIC), operating at its highest CM energy of 5 TeV. This is helped by the robust prediction of the charged and neutral wino mass difference,  $\delta m = 165 - 190$  MeV.
- 4) We have also estimated the monochromatic  $\gamma$ -ray signal coming from the pair annihilation of wino DM at the galactic centre. One finds a viable signal upto wino masses of 2.3 TeV for cuspy DM density profiles.

### Acknowledgments

We thank Manuel Drees, Gian Giudice and Stefano Profumo for many helpful discussions. DPR acknowledges the hospitality of CERN Theory Division, where this work was initiated and receiving partial financial support from BRNS (DAE) under the Raja Ramanna Fellowship Scheme. DD would like to thank the Council of Scientific and Industrial Research, Govt. of India for the support received as a Senior Research Fellow.

## References

- [1] See e.g., Perspectives in Supersymmetry, ed. G.L. Kane, World Scientific (1998); Theory and Phenomenology of Sparticles: M. Drees, R.M. Godbole and P. Roy, World Scientific, Singapore (2005).
- [2] D. Clowe, M. Bradac, A. H. Gonzalez, M. Markevitch, S. W. Randall, C. Jones and D. Zaritsky, arXiv:astro-ph/0608407.

- [3] S. Edelman et al, Review of Particle Properties, *Phys. Lett.* **B592**(2004) 1.
- [4] See e.g., Higgs Boson Theory and Phenomenology: M. Carena and H.E. Haber, *Prog. Part. Nucl. Phys.* **50**(2003) 63.
- [5] N. Arkani-Hamed and S. Dimopoulos, *JHEP* **0506**(2005) 073; G.F. Giudice and A. Romanino, *Nucl. Phys.* **B699**(2004) 65.
- [6] U. Chattopadhyay and P. Nath, *Phys. Rev. D* **66** (2002) 093001.
- [7] A. Masiero, S. Profumo and P. Ullio, *Nucl. Phys. B* **712** (2005) 86.
- [8] N. Arkani-Hamed, A. Delgado and G. F. Giudice, *Nucl. Phys. B* **741** (2006) 108.
- [9] J.L. Feng, K.T. Matchev and F. Wilczek, *Phys. Rev. D* **63**(2001) 045024.
- [10] U. Chattopadhyay, D. Choudhury, M. Drees, P. Konar and D. P. Roy, *Phys. Lett. B* **632** (2006) 114.
- [11] D. N. Spergel *et al.*, arXiv:astro-ph/0603449.
- [12] L. Randall and R. Sundrum, *Nucl. Phys.* **B557**(1999) 79.
- [13] G.F. Giudice, M.A. Luty, H. Murayama, and R. Rattazzi, *J. High Energy Phys.* **12** (1998) 027.
- [14] T. Gherghetta, G.F. Giudice, and J.D. Wells, *Nucl. Phys. B* **559** (1999) 27.
- [15] J. D. Wells, *Phys. Rev. D* **71** (2005) 015013.
- [16] A. Brignole, L. E. Ibanez and C. Munoz, *Nucl. Phys. B* **422** (1994) 125 [Erratum-*ibid. B* **436** (1995) 747];  
J. A. Casas, A. Lleyda and C. Munoz, *Phys. Lett. B* **380** (1996) 59.
- [17] G. Belanger, F. Boudjema, A. Pukhov and A. Semenov, *Comput. Phys. Commun.* **174** (2006) 577 [arXiv:hep-ph/0405253].
- [18] P. Gondolo, J. Edsjo, P. Ullio, L. Bergstrom, M. Schelke and E. A. Baltz, *JCAP* **0407** (2004) 008.

- [19] S. Profumo (Private communication)
- [20] A. Djouadi, J. L. Kneur and G. Moultaka, arXiv:hep-ph/0211331.
- [21] P. Salati, Phys. Lett. **B571**(2003) 121; F. Rosati, Phys. Lett. **B570**(2003) 5.
- [22] B. Murakami and J.D. Wells, Phys. Rev. **D64** (2001) 015001; T. Moroi and L. Randall, Nucl. Phys. **B570**(2000) 455; W.B. Lin, D.H. Huang, X. Zhang and R.H. Brandenburger, Phys. Rev. Lett. **86**, (2001) 954. M. Fujii and K. Hamaguchi, Phys. Lett. **B525**(2002) 143.
- [23] H. Baer, J. K. Mizukoshi and X. Tata, Phys. Lett. B **488** (2000) 367 [arXiv:hep-ph/0007073].
- [24] Physics at the CLIC Multi-TeV Linear Collider: CLIC Physics Working Group, [arXiv:hep-ph/0412251].
- [25] C.H. Chen, M. Drees and J.F. Gunion, Phys. Rev. Lett. **76** (1996) 2002 [arXiv:hep-ph/9512230]; Phys. Rev. D55 (1997) 330 [arXiv:hep-ph/9607421]; Addendum/Erratum [arXiv:hep-ph/9902309].
- [26] OPAL Collab., G.A. Abbiendi et al., Eur. Phys. J. **C29**(2003) 479.
- [27] M. Drees and R.M. Godbole, Z. Phys. **C59**(1993) 591 [arXiv:hep-ph/9203219].
- [28] See e.g., Physics Interplay of the LHC and the ILC: LHC/LC study group, arXiv:hep-ph/0410364.
- [29] J. Hisano, S. Matsumoto, M. M. Nojiri and O. Saito, Phys. Rev. D **71** (2005) 063528.
- [30] D. M. Pierce, J. A. Bagger, K. T. Matchev and R. j. Zhang, Nucl. Phys. B **491** (1997) 3; H. C. Cheng, B. A. Dobrescu and K. T. Matchev, Nucl. Phys. B **543** (1999) 47.
- [31] M. Drees and R.M. Godbole, Phys. Rev. Lett. **67**(1991) 1189.
- [32] L. Bergstrom, P. Ullio and J.H. Buckley, Astropart Phys. **9**(1998) 137 [astro-ph/9712318]; P. Ullio and L. Bergstrom, Phys. Rev. **D57**(1998) 1962.
- [33] J.F. Navarro, C.S. Frenk and S.D.M. White, Astrophys. J. **462**(1996) 563 and **490**(1997) 493.

- [34] J. Diemand, B. Moore and J. Stadel, Mon. Not. Roy. Astron. Soc. **353** (2004) 624 [arXiv:astro-ph/0402267]; B. Moore et al., *Astrophys. J.* **524**(1999) L19.
- [35] A. Burkert, *Astrophys. J.* **447**(1995) L25
- [36] B. Thomas, *Phys. Rev. D* **72** (2005) 023519.
- [37] F. Aharonian *et al.* [The HESS Collaboration], *Astron. Astrophys.* **425** (2004) L13 [arXiv:astro-ph/0408145].
- [38] D. Grasso and L. Maccione, *Astropart. Phys.* **24** (2005) 273 [arXiv:astro-ph/0504323].
- [39] G. Zaharijas and D. Hooper, *Phys. Rev. D* **73** (2006) 103501.